Journal of Sound and Vibration (1999) **228**(5), 977–994
Article No. jsvi.1999.2445, available online at http://www.idealibrary.com on IDEAL®

SENSITIVITY ANALYSIS OF LOCAL/GLOBAL MODAL PARAMETERS FOR IDENTIFICATION OF A CRACK IN A BEAM

K. LAKSHMI NARAYANA AND C. JEBARAJ

AU-FRG Institute for CAD/CAM, Anna University, Madras 600 025, *India*

A crack in a structure will affect the modal parameters both locally as well as globally. The present work discusses the studies carried out using those parameters that get changed locally and globally as well as a procedure to identify the crack location. Even though the crack can be located exactly by monitoring changes that occur in the parameters locally such as strain variation, etc., this method has limitations in terms of extracting these locally varying modal parameters. A new technique is presented to identify the presence of a crack and its location, from the changes that occur in a few of its lowest natural frequencies, one of the modal parameters that changes globally. The study is carried out both analytically and experimentally and the results are presented in this paper. A cantilever beam was considered and modelled with flat plate bending elements so as to introduce the crack and analyze the propagation of the crack. The crack is a through-thickness one, growing along the breadth of the beam starting from one edge. The location of the crack is also moved from the fixed end to the free end along its length. The changes in natural frequencies are observed from analytical study, due to the presence of the crack at different locations and depths, and the percentage change in frequency values are calculated. These results are confirmed by the experiments. From these observations a method is suggested to identify the location of the crack.

1. INTRODUCTION

The development of damage detection techniques for vibrating structures such as aircraft structures, large space structures and structures used in ocean environment has recently become a focus of substantially growing research efforts. The cracks can be present in structures due to their limited fatigue strengths or due to the manufacturing processes. These cracks open for a part of the cycle and close when the vibration reverses its direction. These cracks will grow over time, as the load reversals continue, and may reach a point where they pose a threat to the integrity of the structure. As a result, all such structures must be carefully maintained and monitored so that in the event of development of any crack, it can be located and repaired before it can impair the safety of the structures.

There are several non-destructive testing techniques available for crack detection, for example: Visual examination, Radiographic tests, Ultrasonic testing, Liquid penetrate tests and Magnetic particle tests. All the above methods cannot be

0022-460X/99/500977 + 18 $30.00/0

utilized under operating conditions of the structures. Due to this limitation it is now believed that the monitoring of the global dynamics of structures offers promising alternatives for damage detection. The modal parameters such as natural frequencies and mode shapes can be used to detect the initiation and development of fatigue cracks. In this present work, we have used the changes in natural frequencies only, to locate the crack in a cantilever beam.

2. A BRIEF LITERATURE SURVEY

A lot of work has been done and reported in the literature in the area of sensitivity analysis of modal parameters due to the presence of a crack in simple structures like beams. Adams *et al.* [1] modelled the presence of a crack as a spring whose stiffness got reduced and also measured the frequency variations. They modelled the structure as one dimensional and suggested a closed-form procedure to identify the presence/absence of a crack. Later Cawley and Adams [2] extended the same procedure to two dimension and proposed a method to monitor the growth of damage.

Chondros and Dimarogonas [3] modelled the crack in a welded joint replacing it by a torsional spring and carried out an analytical solution procedure. The results were plotted as changes in frequency of the structure related to the depth of the crack. However, they stated that caution must be exercised concerning the material properties of the weld and also the changes in material properties that occur while in service. Gudmundson [4] proposed a theoretical procedure to predict the crack length, the crack position and the crack orientation, and the measured eigenfrequency changes were used as input data. The analytical eigenvalue change was measured using fracture mechanics approach in terms of crack length, the crack position and crack orientation. The difference in the measured and analytical eigenvalues was termed as error function and minimization of that error function identified the location of the crack. Ostachowicz and Krawczuk [5] proposed a procedure for identification of a crack based on the measurement of the deflection shape of the beam. Gounaris and Dimarogonas [6] and Qian *et al.* [7] formulated an algorithm using finite element method to model a cracked beam. An element stiffness matrix of a beam with a crack was formulated and then a finite element model of a cracked beam was developed. It was observed that the vibration amplitudes were affected considerably by the presence of cracks. However, it is very difficult to measure slopes on the structures although a laser beam technique could be used.

Abraham and Brandon [8] used substructure normal modes to predict the vibration responses of a cantilever beam with a breathing transverse crack. Pandey *et al.* [9] suggested another parameter, namely curvature of the deflected shape of beam instead of change in frequencies to identify the location of the crack. Rizos *et al.* [10] measured the amplitude at two points and proposed an algorithm to identify the location of the crack. Feng *et al.* [11] have suggested measurement of strain in the cracked beam and stated that strain mode was more sensitive to the damage of the structure than the natural frequency. Swamidas and Chen [12] compared a lot of their experimental work with analytical work and concluded that the sensitive parameters affected by a crack in the beam were the natural frequencies, response amplitudes and mode shapes. However, the most sensitive parameter was the the difference of strain mode shapes and local strain frequency response functions.

Ratcliffe [13] used a modified Laplacian operator on mode shape data to locate the damage in a beam. But it requires cumbersome post processing of determining cubic polynomial to fit the Laplacian locally at each spatial co-ordinate. The theory of spring-loaded fracture-hinge was used by Ju and Mimovich [14] to diagnose the fracture damage in structures by post processing the experimentally obtained frequency values with analytical frequency equations. Tasi and Wang [15] used the change in fundamental mode shapes between the cracked and uncracked shafts to identify the crack location. The crack was modelled as a joint of a local spring. The transfer-matrix method was employed to obtain the dynamic characteristics. A bilinear device was used by Chance *et al.* [16] to simulate the crack in beams and plates by using mode shapes and curvatures to locate a crack.

In the brief review presented above, it is observed that the prediction of the exact crack location and the prediction of the severity of the crack are still elusive. Hence an attempt has been made in this study to address these issues and a procedure proposed for the prediction of the same.

3. THEORETICAL BACK GROUND

3.1. FLEXURAL VIBRATION OF A BEAM

The partial differential equation of motion for the forced vibration of a non-uniform beam is

$$\frac{\partial^2}{\partial x^2}\left[EI(x)\frac{\partial^2 w(x,t)}{\partial x^2}\right] + \rho A(x)\frac{\partial^2 w(x,t)}{\partial t^2} = f(x,t), \tag{1}$$

For free vibration $f(x,t) = 0$, and hence the equation of motion becomes

$$\frac{\partial^2}{\partial x^2}\left[EI(x)\frac{\partial^2 w(x,t)}{\partial x^2}\right] + \rho A(x)\frac{\partial^2 w(x,t)}{\partial t^2} = 0, \tag{2}$$

Solving of the above equation is equivalent to solving of the stationary value of the variation of the equation:

$$\omega^2 = \lambda = \frac{\int_0^l EI(x)\{\mathrm{d}^2 w/\mathrm{d}x^2\}^2\,\mathrm{d}x}{\int_0^l mw(x)^2\,\mathrm{d}x} = \frac{U}{V}, \tag{3}$$

where $m = \rho A(x)$, for non-uniform cross-section.

Taking variation for both sides of equation (3), we get

$$\partial\lambda = \frac{\partial U}{V} - \frac{U\partial V}{V^2}, \tag{4}$$

Dividing both sides of equation (4) by λ, we get

$$\frac{\partial\lambda}{\lambda} = \frac{\partial U}{U} - \frac{\partial V}{V} \tag{5}$$

for a very small crack in beam $\delta m = 0 \Rightarrow \delta V = 0$:

$$\frac{\partial \lambda}{\lambda} = \frac{\partial U}{U} = \frac{E\partial\left[\int_0^l I(x)\,\{\mathrm{d}^2 w/\mathrm{d}x^2\}^2\,\mathrm{d}x\right]}{E\int_0^l I(x)\,\{\mathrm{d}^2 w/\mathrm{d}x^2\}^2\,\mathrm{d}x}, \tag{6}$$

considering the numerator of equation 6, viz,

$$\partial U = \partial\left[\int_0^l EI\{\mathrm{d}^2 w/\mathrm{d}x^2\}^2\,\mathrm{d}x\right].$$

Let the crack be at the location l_0 with a width Δx. Then we can write the above equation as

$$\partial U = \partial\left[\int_0^{l_0} EI\left\{\frac{\mathrm{d}^2 w}{\mathrm{d}x^2}\right\}^2 \mathrm{d}x + \int_{l_0}^{l_0+\Delta x} EI\left\{\frac{\mathrm{d}^2 w}{\mathrm{d}x^2}\right\}^2 \mathrm{d}x + \int_{l_0+\Delta x}^{l} EI\left\{\frac{\mathrm{d}^2 w}{\mathrm{d}x^2}\right\}^2 \mathrm{d}x\right], \tag{7}$$

Since there is insignificant change in curvature, from 0 to l_0 and $(l_0 + \Delta x)$ to l, the first and the last terms of the above equation will be zero, then

$$\partial U = \partial\left[0 + \int_{l_0}^{l_0+\Delta x} EI\left\{\frac{\mathrm{d}^2 w}{\mathrm{d}x^2}\right\}^2 \mathrm{d}x + 0\right]$$

$$\partial U = E\left[\int_{l_0}^{l_0+\Delta x} \partial I\left\{\frac{\mathrm{d}^2 w}{\mathrm{d}x^2}\right\}^2 \mathrm{d}x + \int_{l_0}^{l_0+\Delta x} I\cdot\partial\left\{\left(\frac{\mathrm{d}^2 w}{\mathrm{d}x^2}\right)^2 \mathrm{d}x\right\}\right]$$

$$= EI\left[\frac{\partial I}{I}\cdot\int_{l_0}^{l_0+\Delta x}\left\{\frac{\mathrm{d}^2 w}{\mathrm{d}x^2}\right\}^2 \mathrm{d}x + \int_{l_0}^{l_0+\Delta x}\partial\left\{\frac{\mathrm{d}^2 w}{\mathrm{d}x^2}\right\}^2 \mathrm{d}x\right]. \tag{8}$$

For a rectangular beam of width "B" and thickness "T", $I = BT^3/12$,

$$\partial I = \frac{T^3}{12}\,\partial B \Rightarrow \frac{\partial I}{I} = \frac{\partial B}{B}. \tag{9}$$

Since the integration limit is for a small width of Δx only, equation (8) could be written as

$$\partial U = EI\left[\frac{\partial B}{B}\left\{\frac{\mathrm{d}^2 w}{\mathrm{d}x^2}\right\}^2 \Delta x + \partial\left\{\frac{\mathrm{d}^2 w}{\mathrm{d}x^2}\right\}^2 \Delta x\right]$$

$$= EI\left\{\frac{\mathrm{d}^2 w}{\mathrm{d}x^2}\right\}^2_{at\,\ldots\,l_0} \Delta x\left[\frac{\partial B}{B} + \frac{\partial\{\mathrm{d}^2 w/\mathrm{d}x^2\}^2_{at\,\ldots\,l_0}}{\{\mathrm{d}^2 w/\mathrm{d}x^2\}^2_{at\,\ldots\,l_0}}\right], \tag{10}$$

$$\frac{\partial\lambda}{\lambda}=\frac{\partial U}{U}=\frac{\{\mathrm{d}^2w/\mathrm{d}x^2\}^2_{at\,...\,l_0}\,\Delta x}{\int_0^l\{\mathrm{d}^2w/\mathrm{d}x^2\}^2\,\mathrm{d}x}\left[\frac{\partial B}{B}+\frac{\partial\{\mathrm{d}^2w/\mathrm{d}x^2\}^2_{at\,...\,l_0}}{\{\mathrm{d}^2w/\mathrm{d}x^2\}^2_{at\,...\,l_0}}\right], \tag{11}$$

The above equation (11) indicates that the vibration of the frequency parameter λ is a function of square of transverse strain of the beam at the crack location. Also, it is a function of the variation of beam width and variation of the square of transverse strain at the crack location. Thus, it indicates that the variation of the frequency parameter is a non-linear one.

3.2. TORSIONAL VIBRATION OF A BEAM

The equation of motion for the free vibration of a beam for its torsional oscillation about its own axis is given by

$$GJ\,\frac{\partial^2\theta(x,t)}{\partial x^2}=J_0\,\frac{\partial^2\theta(x,t)}{\partial t^2}. \tag{12}$$

Solving the variation equation of the above problem will yield the following equation:

$$\omega^2=\lambda=\frac{\int_0^l GJ\{\mathrm{d}\theta/\mathrm{d}x\}^2\,\mathrm{d}x}{\int_0^l J_0\theta^2\,\mathrm{d}x}. \tag{13}$$

Similar to equation (11) we can write the variation of the above equation as

$$\frac{\partial\lambda}{\lambda}=\frac{\partial U}{U}=\frac{\{\mathrm{d}\theta/\mathrm{d}x^2\}^2_{at\,...\,l_0}\,\Delta x}{\int_0^l\{\mathrm{d}\theta/\mathrm{d}x\}^2\,\mathrm{d}x}\left[\frac{\partial B}{B}+\frac{\partial\{\mathrm{d}\theta/\mathrm{d}x\}^2_{at\,...\,l_0}}{\{\mathrm{d}\theta/\mathrm{d}x\}^2_{at\,...\,l_0}}\right], \tag{14}$$

Equation (14) indicate that the variation of the frequency parameter λ is a function of square of the torsional strain of the beam at the crack location.

4. EFFECTS ON LOCAL MODAL PARAMETERS DUE TO CRACK

The crack in the structure adds flexibility to the structure. This flexibility will affect the physical properties, like stiffness in the local area around the crack, more than any other area of the structure. Since modal parameters represent the structural properties, monitoring of the local changes in the modal parameters will give a more direct and significant indication of the crack occurring in the structure. The modal parameters that change locally are mode shapes, i.e., bending mode shape, torsional mode shape and strain mode shape.

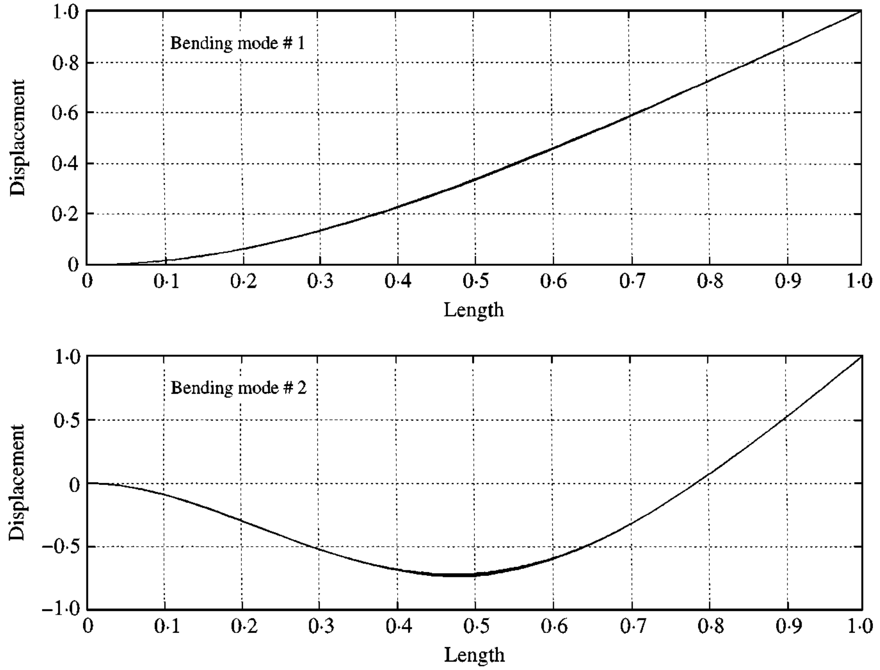

Figure 1. Bending mode shape of uncracked and cracked cantilever beam. (crack location at 0·5L; crack depth from 0·1B to 0·5B).

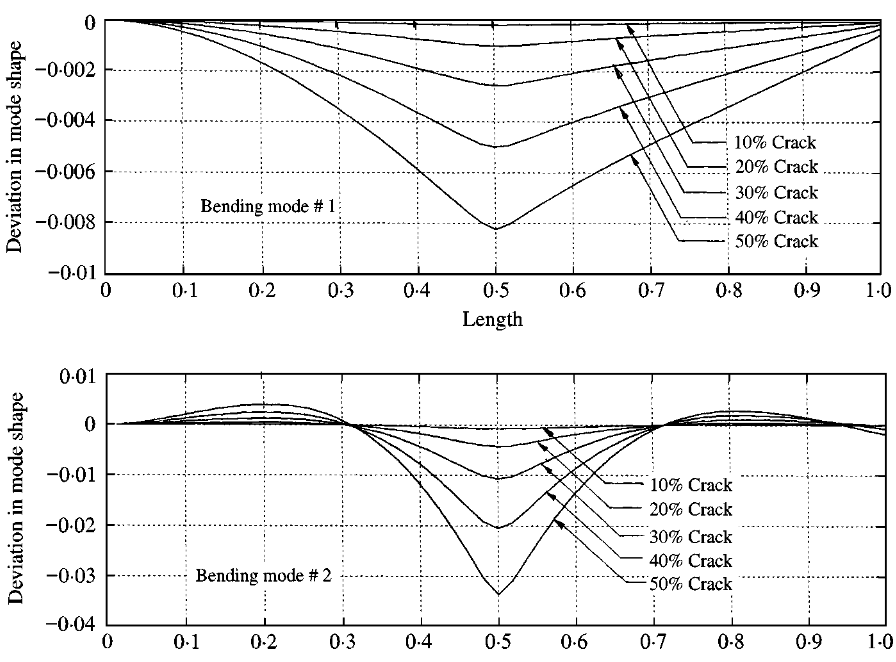

Figure 2. Deviation in bending mode shape of cracked beam w.r.t. uncracked cantilever beam (crack location at 0·5L; crack depth from 0·1B to 0·5B).

4.1. BENDING MODE SHAPE

The flexural mode shape of a uncracked cantilever type of structure is obtained by solving equation (2) with appropriate boundary conditions and is given by

$$w_n(x) = \{\cos(\beta_n x) - \cosh(\beta_n x)\} + \frac{\sin(\beta_n l) - \sinh(\beta_n l)}{\cos(\beta_n l) + \cosh(\beta_n l)}\{\sin(\beta_n x) - \sinh(\beta_n x)\}. \tag{15}$$

However, the theoretical equation (15) representing the mode shape cannot account for the presence of a crack. Hence, it is resolved to approach the problem of accounting for the crack in the structure by using FE technique.

A cantilever beam of the dimensions $L:B:T$ with ratio 50:8:1 of aluminium material was considered for the numerical studies. The beam was modelled with four noded shell elements so as to introduce the crack and analyze for the propagation of the crack. The general purpose FE analysis software ANSYS was used in the modal analysis module to obtain mode shapes.

Mode shape and deviation in the mode shape due to crack for the first and second bending modes are shown in Figures 1 and 2 for the variation of crack depth ranging from 10 to 50% while the crack was located at $L/2$. It is observed that the deviation in mode shape is quite insignificant with maximum deviation value as low as 0·008 and 0·03 as shown in Figure 2, and the deviation is maximum at the crack location. The deviation of the mode shape (deflection) is distributed throughout the span of the beam.

4.2. TORSIONAL MODE SHAPE

The torsional mode shape equation of uncracked beam is obtained by solving equation (12) with appropriate boundary conditions and is given as

$$\theta_n(x) = \sin\left\{\left(\frac{n-1}{2}\right)\cdot\left(\frac{\pi x}{l}\right)\right\}. \tag{16}$$

The same FE mesh as described above was used to obtain the torsional mode shapes. First and second rotational mode shape of a cantilever beam and the changes that occur in the mode shape due to the presence of the crack, ranging from 10 to 50%, are shown in Figure 3, and the maximum deviation in mode shape values are computed and plotted in Figure 4. It is observed that the deviation is as small as 0·0075 and 0·018, and at the location of the crack there is a distinct variation of the change of slope in these curves. Even though there is a qualitative variation in rotational mode shape, the magnitude of this variation is quite insignificant and the physical measurement of this small variation is next to impossible.

4.3. STRAIN MODE SHAPE

The strain mode shapes are the function of second derivatives of the deflected shapes shown in equations (15) and (16). First and second bending stain modes with

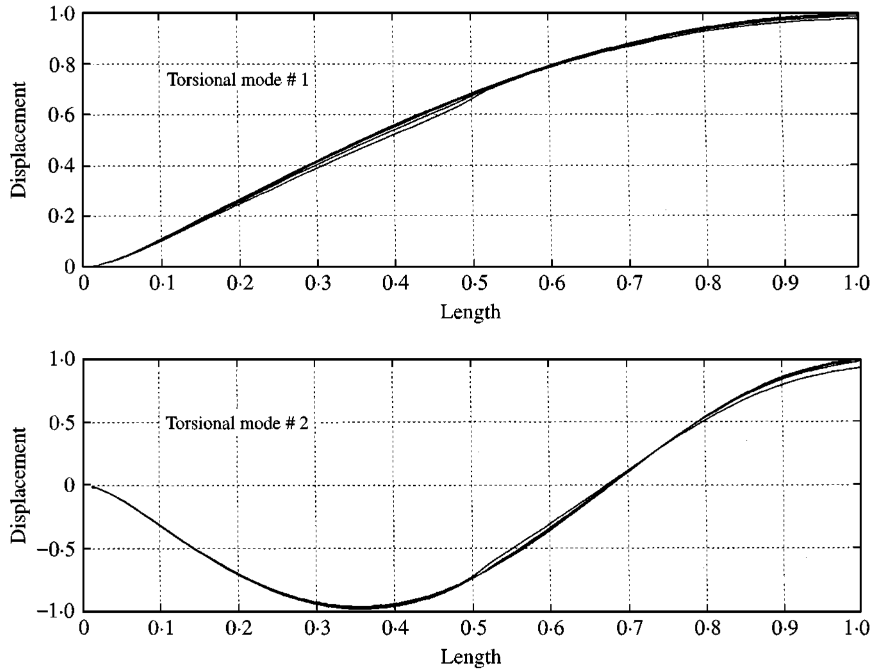

Figure 3. Torsional mode shape of uncracked and cracked cantilever beam (crack location at 0·5L; crack depth from 0·1B to 0·5B).

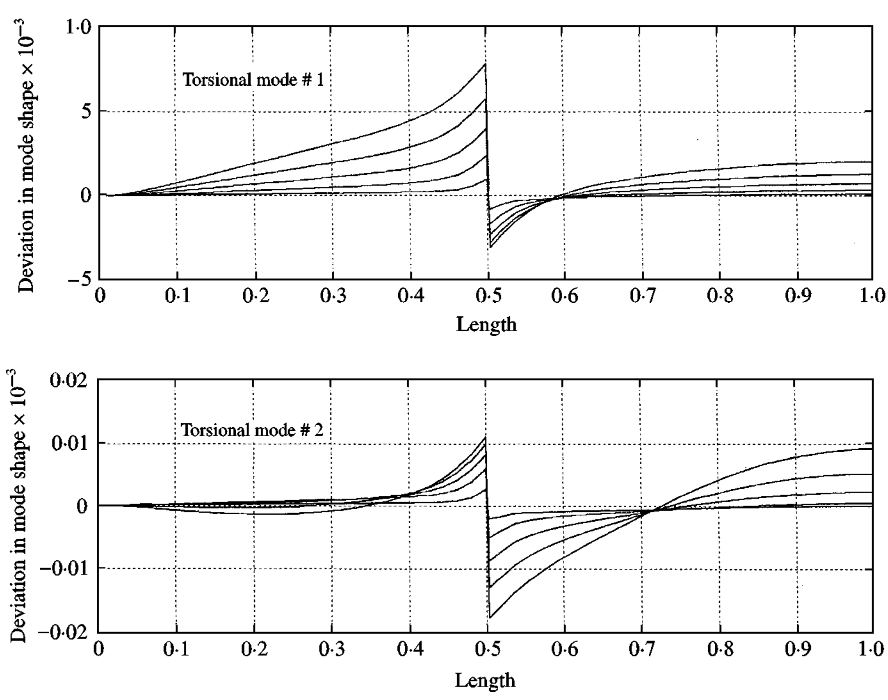

Figure 4. Deviation in torsional mode shape of cracked beam w.r.t. uncracked cantilever beam (crack location at 0·5L; crack depth from 0·1B to 0·5B).

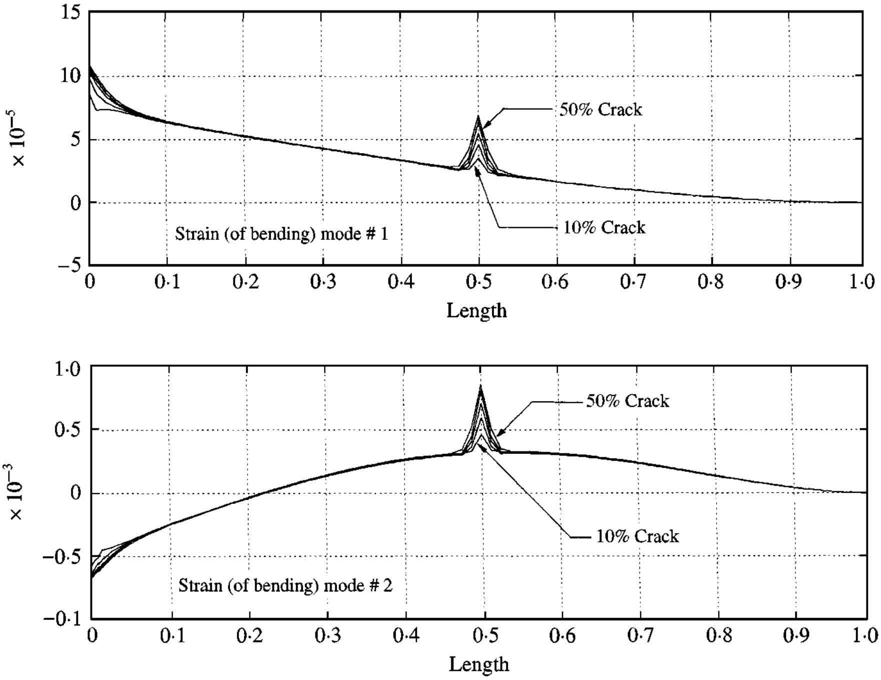

Figure 5. Strain (of bending) mode shape of cracked cantilever beam (crack location at $0{\cdot}5L$; crack depth from $0{\cdot}1B$ to $0{\cdot}5B$).

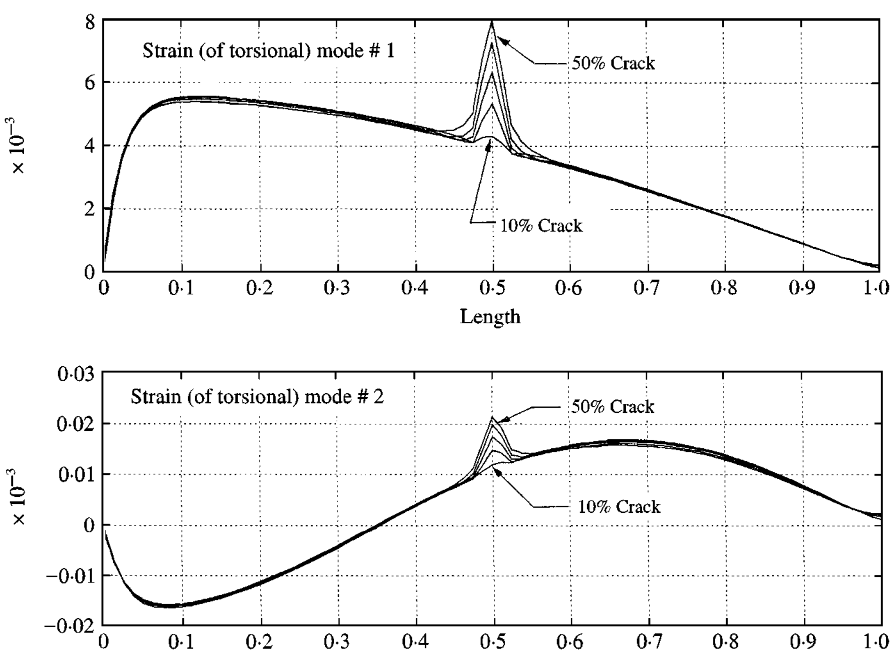

Figure 6. Strain (of torsional) mode shape of cracked cantilever beam (crack location at $0{\cdot}5L$; crack depth from $0{\cdot}1B$ to $0{\cdot}5B$).

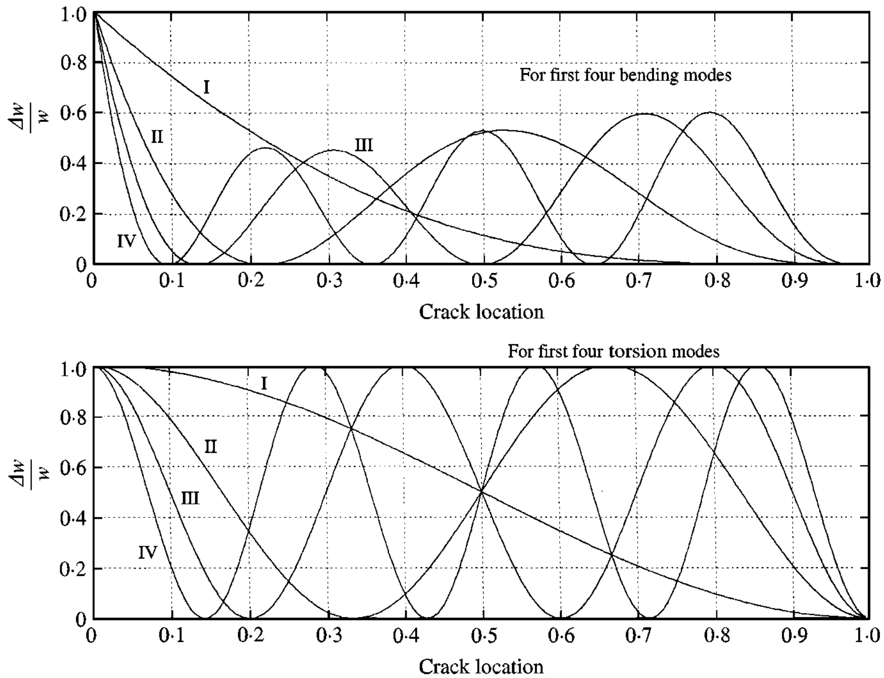

Figure 7. Change in frequency versus crack location of cantilever beam (first four bending and four torsional modes).

the effect of the crack are shown in Figure 5. It is observed that there is quite a significant change in strain modes at the location of the crack. However, this change is quite localized, namely, in the vicinity of the crack only. Therefore, measurement of strain by a sensor at the crack location would be ideal but all other places the sensor will not have any sensible variation. Therefore, measurement of strain mode values is not a practical one to locate the crack since prior knowledge of the location of the crack is not available to us.

Similarly, the first and second torsional strain modes are shown in Figure 6. We could observe a similar behavior as above, i.e., there is a steep variation in strain at the crack location. The limitation to measure the strain at the location of the crack prevails here also.

4.4. EFFECT OF USE OF LOCAL/GLOBAL MODAL PARAMETERS TO LOCATE THE CRACK

The discussions in the previous three sections indicate that the local parameters like bending and torsional mode deviation and strain mode changes have insignificant contribution or highly localized contribution which cannot be practically measured to identify the location of the crack. Therefore, an attempt is made to look into the global parameters, like frequencies and the change in frequencies, to identify the presence of a crack.

The change in frequency of any mode is dependent on the location and depth of crack, and it is proportional to the square of the strain value of that mode at a particular location [equations (11) and (14)]. In other words, the change in

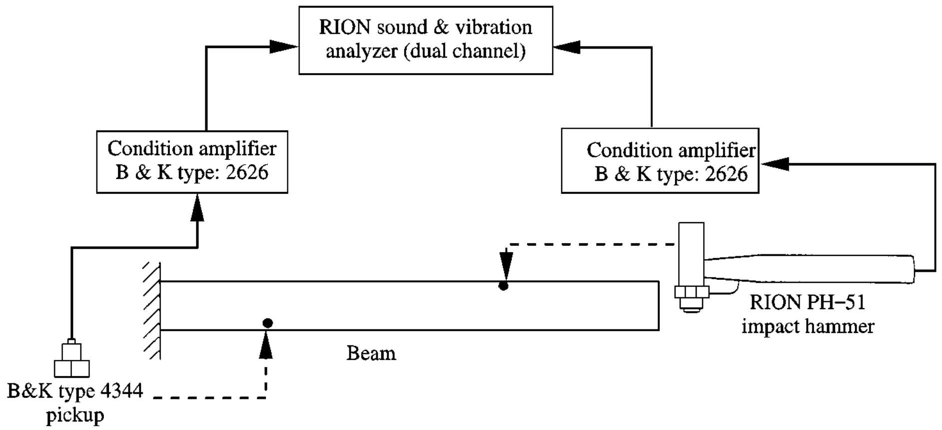

Figure 8. Experimental setup.

frequency is maximum if the crack is located at the peak/trough of the strain mode, and it is minimum if the crack is located at the node of the strain mode. Equations (11) and (14) are plotted and shown in Figure 7 by normalizing the maximum value (at the fixed end) to unity.

In the next section, a study is made to compare the change in frequencies, obtained due to the presence of a crack, in a beam with an uncracked beam. Both experimental as well as analytical work was carried out, and the results obtained are tabulated, plotted and discussed.

5. EVALUATION OF FREQUENCY CHANGES

The procedure used to evaluate the variation of frequency change should be identical when it is verified by two different procedures, namely, experimental and analytical. In the present work both the experimental as well as the numerical (FEM) procedures are used to estimate the frequency changes before they are compared.

5.1. EXPERIMENTAL PROCEDURE

The same aluminium beam of the dimensions $L:B:T$ with ratio 50:8:1 is considered for the experiment. RION SA-73 Sound and Vibration Dual Channel analyzer is used, to extract the natural frequencies, along with B&K-Type 4344 pickup and RION PH-51 impact hammer. Only a few of the lower order frequencies, including the fundamental frequency, were extracted from the experiment.

To start with, the natural frequencies of the uncracked cantilever beam were measured. Then the crack was generated and propagated to the desired width by a thin saw cut (around 0·8 mm thick). Nine specimens with the same geometry, material and cracked at $0{\cdot}1L$ to $0{\cdot}9L$, with an increment of $0{\cdot}1L$, from the clamped end, and with crack depths of $0{\cdot}1B$ to $0{\cdot}5B$, with an increment of $0{\cdot}1B$, at each

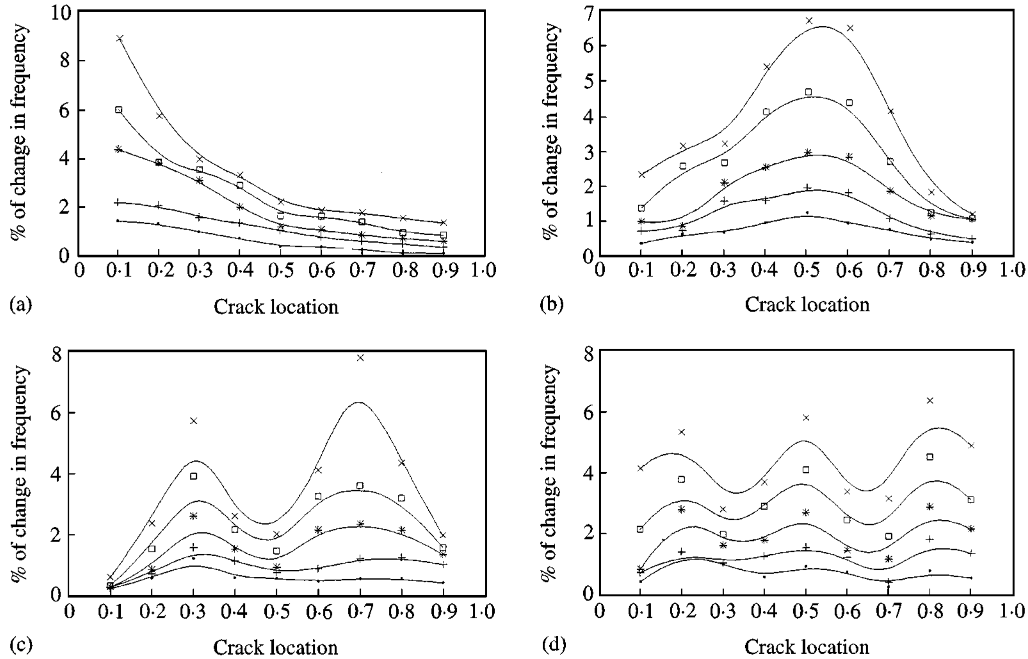

Figure 9. Percentage of change in first four bending frequencies due to a crack. Experimental results (Mesh configuration 1). (a). I bending mode; (b) II bending mode; (c) III bending mode; (d) IV bending mode. —●— 1/10th crack; —+—; 2/10th crack; —∗—; 3/10th crack; —□— ; 4/10th crack; —×— 5/10th crack.

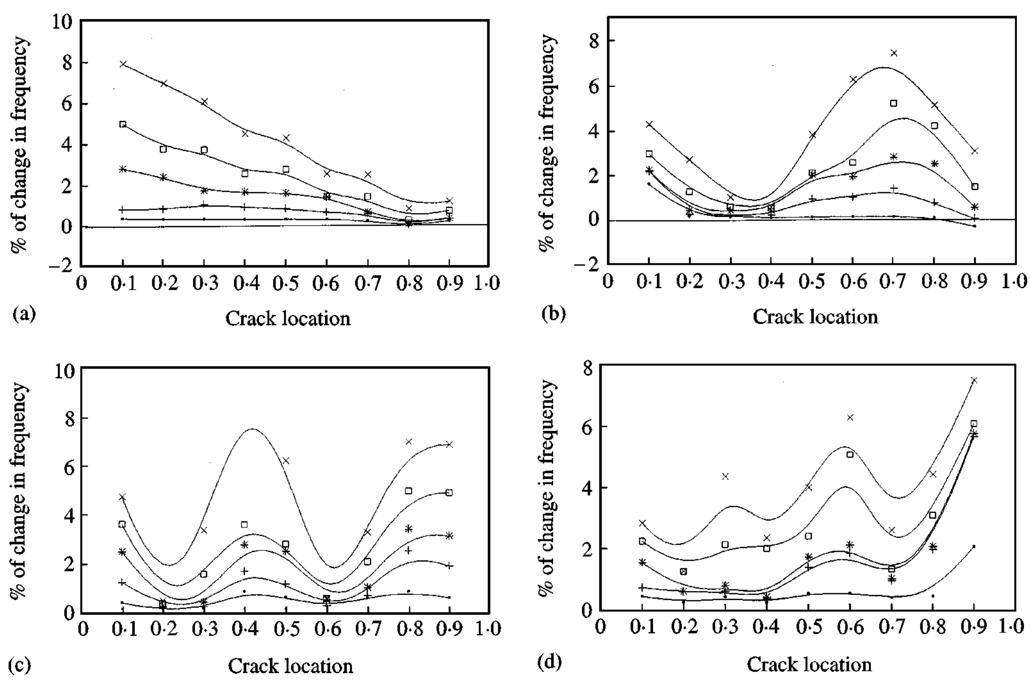

Figure 10. Percentage of change in first four torsional frequencies due to a crack. Experimental results (Mesh configuration 1). (a) I torsional mode; (b) II torsional mode; (c) III torsional mode; (d) IV Torsional mode. —●— 1/10th crack; —+—; 2/10th crack; —∗—; 3/10th crack; —□— ; 4/10th crack; —×—5/10th crack.

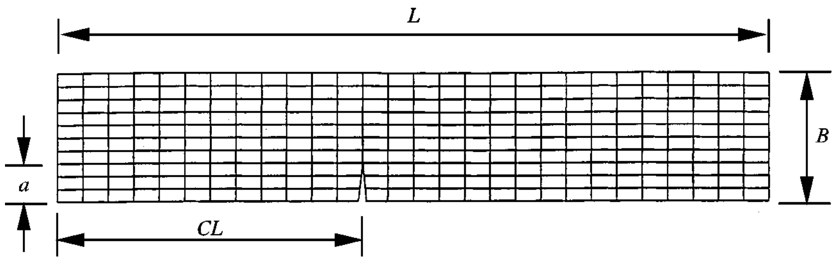

Figure 11. FE mesh of cracked beam. L = length of beam; a = crack depth; B = width of beam; CL = crack location.

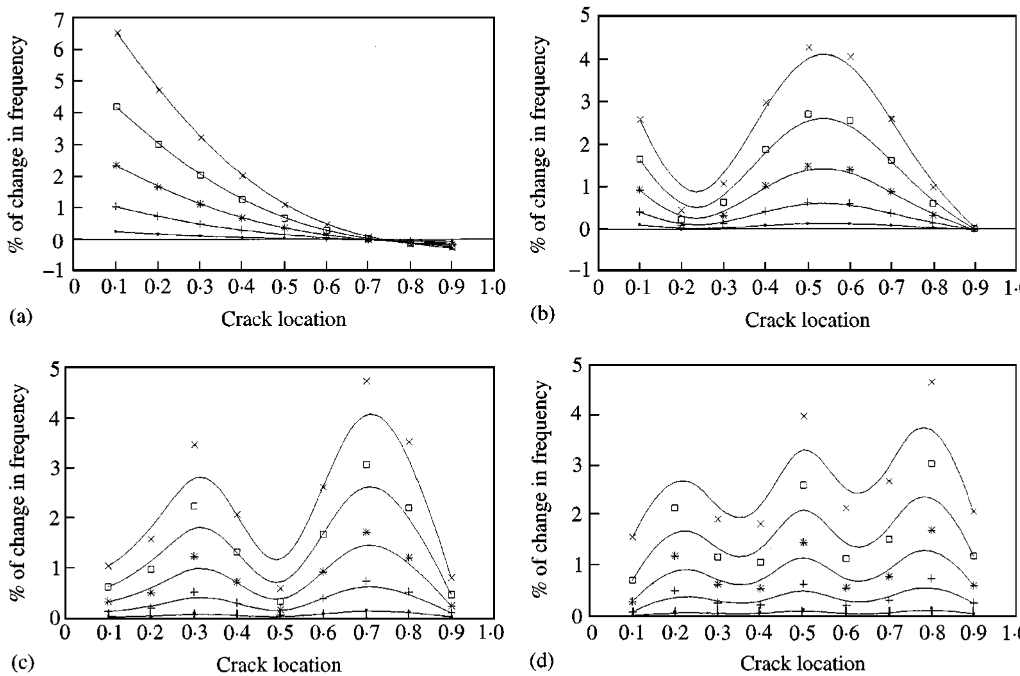

Figure 12. Percentage of change in first four bending frequencies due to a crack. Analytical results (Mesh configuration 1). I bending mode; (b) II bending mode; (c) III bending mode; (d) IV bending mode. —●— 1/10th crack; —+—; 2/10th crack; —*—; 3/10th crack; —□— ; 4/10th crack; —×— 5/10th crack.

location were tested. The "ZOOMING" capability of the analyzer was used to observe the change in frequency as crack depth increased.

From experimentally measured frequency values the percentage of change in the first four bending and the first four torsional frequencies with respect to the uncracked beam for each crack location and depth are calculated and shown in Figures 9 and 10. These results are compared with the analytical finite element results and discussed in the next section.

5.2. ANALYTICAL PROCEDURE

A cantilever beam with the same size and material properties was considered for the numerical studies using ANSYS software. The FE mesh, with the crack

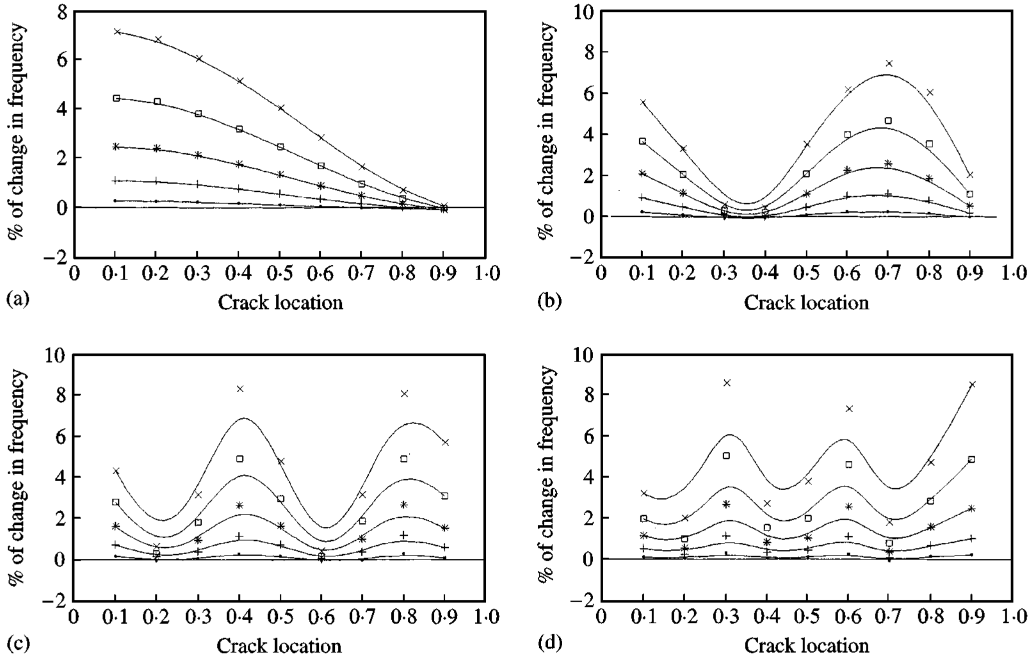

Figure 13. Percentage of change in first four torsional frequencies due to a crack. Analytical results (Mesh configuration 1). (a) I Torsional mode; (b) II Torsional mode; (c) III Torsional mode; (d) IV Torsional mode. —●— 1/10th crack; —+—; 2/10th crack; —∗—; 3/10th crack; —⊟— ; 4/10th crack; —×— 5/10th crack.

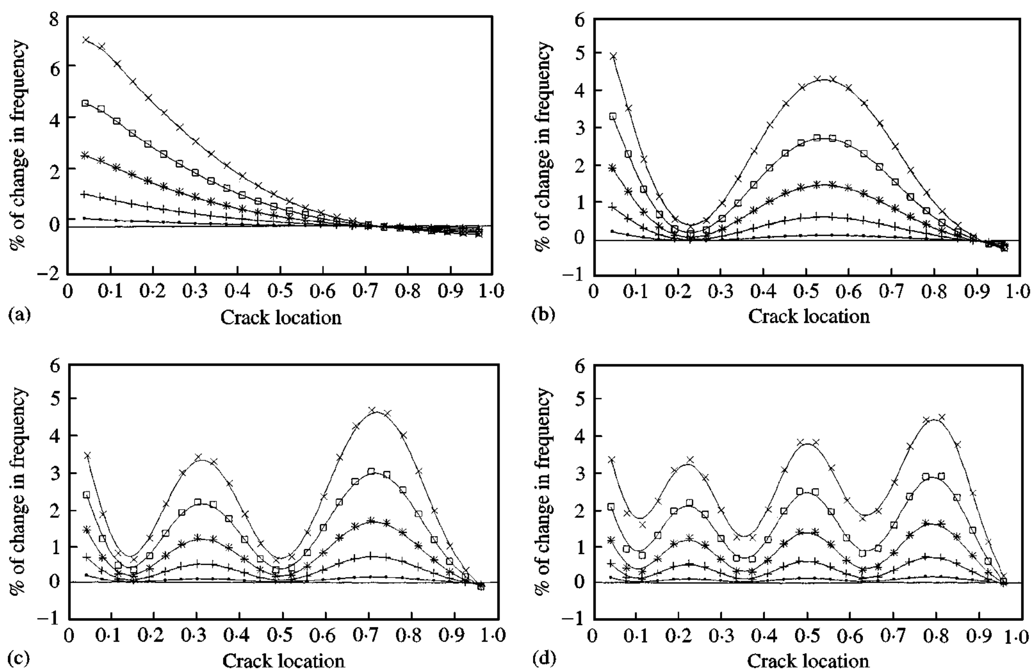

Figure 14. Percentage of change in first four bending frequencies due to a crack. Analytical results (Mesh configuration 2). (a). I bending mode; (b) II bending mode; (c) III bending mode; (d) IV bending mode. —●— 1/10th crack; —+—; 2/10th crack; —∗—; 3/10th crack; —⊟— ; 4/10th crack; —×— 5/10th crack.

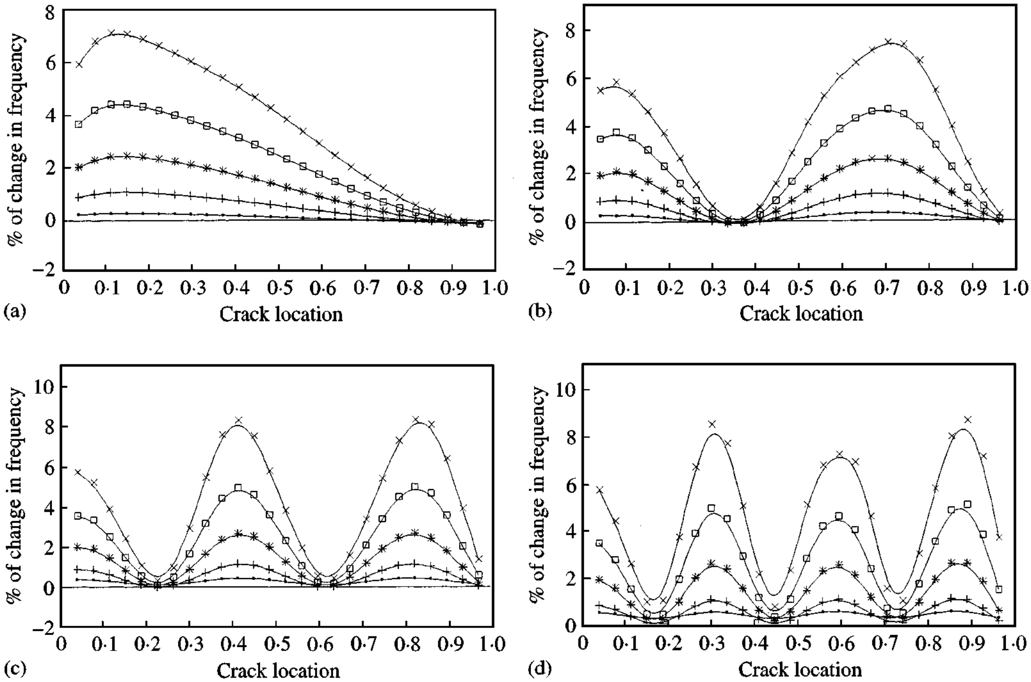

Figure 15. Percentage of change in first four torsional frequencies due to a crack. Analytical results (Mesh configuration 2). (a) I Torsional mode; (b) II Torsional mode; (c) III Torsional mode; (d) IV Torsional mode. —●— 1/10th crack; —+—; 2/10th crack; —*—; 3/10th crack; —□— ; 4/10th crack; —×— 5/10th crack.

TABLE 1

Peak/trough and node locations of strain mode shapes

Mode	Peak/trough loation (s)	Node locations (s)
Bending mode #1	$0{\cdot}0L$	$1{\cdot}0L$
Bending mode #2	$0{\cdot}0L$, $0{\cdot}5287L$	$0{\cdot}2175$, $1{\cdot}0L$
Bending mode #3	$0{\cdot}0L$, $0{\cdot}3075L$, $0{\cdot}7087L$	$0{\cdot}1325L$, $0{\cdot}4907L$, $1{\cdot}0L$
Bending mode #4	$0{\cdot}0L$, $0{\cdot}22L$, $0{\cdot}5L$, $0{\cdot}795L$	$0{\cdot}0945L$, $0{\cdot}356L$, $0{\cdot}6416L$, $1{\cdot}0L$
Torsional mode #1	$0{\cdot}0L$	$1{\cdot}0L$
Torsional mode #2	$0{\cdot}0L$, $0{\cdot}6667L$	$0{\cdot}3333L$, $1{\cdot}0L$
Torsional mode #3	$0{\cdot}0L$, $0{\cdot}4L$, $0{\cdot}8L$	$0{\cdot}2L$, $0{\cdot}6L$, $1{\cdot}0L$
Torsional mode #4	$0{\cdot}0L$, $0{\cdot}285L$, $0{\cdot}5725L$, $0{\cdot}8775L$	$0{\cdot}1425L$, $0{\cdot}4275L$, $0{\cdot}7125L$, $1{\cdot}0L$

nomenclature, is shown in Figure 11. Only the first four bending modes and first four torsional modes was extracted which were adequate to identify the crack location. The analysis was carried out for two types of mesh configurations and are described below.

Mesh Configuration—1: Initially, the crack location and length considered were the same as those of the experimental ones, i.e., the crack location was moved from $0{\cdot}1L$ to $0{\cdot}9L$ with an increment of $0{\cdot}1L$ along the length with crack depth varying from $0{\cdot}1B$ to $0{\cdot}5B$ with an increment of $0{\cdot}1B$, for every crack location, across the width of the beam. The percentage change in frequencies, due to crack, for different crack locations and depths were calculated and are presented in Figures 12 and 13. These numerical results were compared with the theoretical results of equations (11) and (14) presented in Figure 7. It is observed that the numerical results agree qualitatively with the theoretical results.

Mesh Configuration—2: Due to increasing confidence in the procedure, the FE analysis was extended to more crack locations to observe the change in frequencies as the crack moves in closely spaced intervals. In this analysis, the crack location was assumed to move from $0{\cdot}04L$ to $0{\cdot}96L$ with an increment of $0{\cdot}04L$ along the length. The depth of the crack at each crack location was assumed to vary from $0{\cdot}1B$ to $0{\cdot}5B$ with an increment of $0{\cdot}1B$ across the depth of the beam. The percentage change in frequencies, for different crack locations and depths were calculated and presented in Figures 14 and 15. On comparing these results with the theoretical results presented in Figure (7), it is observed that the agreement is much better for this mesh configuration.

6. DISCUSSIONS

In general, it was observed that for all four bending and torsional modes the absolute percentage of change in frequency values increased as depth of the crack increased.

Mesh Configuration-1: Both experimental and analytical studies were carried out for mesh configuration 1. Figures 9 and 10 are compared with Figures 12 and 13 and it is observed that the percentage change in frequency values were slightly higher in the case of experiments. But the percentage change in frequency values as the crack moved along the length showed the same qualitative trend in experimental and analysis results. Thus, the experimental study validated the FE model results.

Mesh Configuration-2: It is observe that the percentages of change in frequency values were different for different crack locations as shown in the plots. As the crack location moved from the clamped end to the free end, it was observed that the percentage change in frequency values, shown in Figures 14 and 15, is similar to the square of the strain values shown in Figure 7 representing equations (11) and (14). Therefore, it can be concluded from these observations that:

(I) If the crack is located at the peak/trough positions of the strain mode shapes, then the percentage change in frequency values would be higher for corresponding modes.

(II) If the crack is located at the nodal points of the strain mode shapes, then the percentage change in frequency values would be lower for corresponding modes.

Thus, the above observation and discussions are in conformity with equations (11) and (14).

Considering the lowest four bending strain modes, there are seven peaks/troughs and seven nodes as listed in Table 1 above. Therefore, we can locate the crack as that present in the vicinity of any one of the 14 locations. Similarly, we could locatethe crack in the vicinity of 14 such locations obtained for torsional strain

TABLE 2

Percentage change in frequency due to crack

Mode no.	Percentage of change in frequency	
	Bending modes	Torsional modes
I	0·1697	2·0114
II	3·1704	7·0786
III	4·2831	1·5722
IV	1·9605	4·6405

modes. Thus accuracy of the prediction will be approximately $L/28$, as illustrated in the case study shown in Section 7 below.

7. CRACK IDENTIFICATION—A CASE STUDY

As a case study, the percentage change in frequencies for a cantilever beam observed/measured for a particular case is presented in Table 2.

From the above data, we know that the maximum percentage of change in frequency among the bending modes in III mode. From our observations and conclusions I & II made in section 6, we can say that the crack would be nearer to $0{\cdot}0L$ (clamped end) or $0{\cdot}3075L$ or $0{\cdot}7087L$ (peak/trough of III bending strain mode shape). Maximum percentage change in frequency among the torsional modes is II mode. This implies that, from our observation (section 6), the crack will be nearer to $0{\cdot}0L$ or $0{\cdot}6667L$ (peak of II torsional strain mode shape). The crack is not located near the clamped end because the change in I bending and torsional mode is much less. Therefore, we can conclude that the crack location will be between $0{\cdot}7087L$ and $0{\cdot}666L$ from the clamped end. The exact location of the crack is $0{\cdot}67L$ for 50% crack depth. Thus, the prediction based on the case study results matches closely with the exact crack location.

8. CONCLUSION

The results of the present work have indicated that local modal parameters such as mode shape and variation in mode shape are not good enough for identifying the location of the crack. The change in frequencies of a few of the fundamental modes is a valid global parameter for identifying the location of the crack. These changes in frequency values, in real application, can be obtained by monitoring the frequencies measured periodically by sensors mounted in the structure at the time of installation.

In this study even though we considered a simple structure, we can extend the same procedure to identify and locate cracks in complex structures.

REFERENCES

1. R. D. ADAMS, P. CAWLEY, C. J. PYE and B. J. STONE 1978 *Journal of Mechanical Engineering Science* **20**, 93–100. A vibration technique for non-destructively assessing the integrity of structures.
2. P. CAWLEY and R. D. ADAMS 1979 *Journal of Strain Analysis* **14**, 49–57. The location of defects in structures from measurements of natural frequencies.

3. T. G. Chondros and A. D. Dimarogonas 1980 *Journal of Sound and Vibration* **69**, 531–536. Identification of crack in welded joints of complex structures.
4. P. Gumundson 1984 *Proceedings of the II International Modal Analysis Conference*, 690–697. Changes in modal parameters resulting from small cracks.
5. W. M. Ostachowicz and M. Krawczuk 1990 *Computers and Structures* **36**, 245–250. Vibration analysis of a cracked beam.
6. G. Gounaris and A. Dimarogonas 1988 *Computers and Structures* **28**, 309–313. A finite element of a cracked prismatic beam for structural analysis.
7. G. L. Qian, S. N. Gu and J. S. Jiang 1990 *Journal of Sound and Vibration* **138**, 233–243. The dynamic behaviour and crack detection of a beam with a crack.
8. O. N. L. Abraham and J. A. Brandon 1995 *ASME Journal of Vibration and Acoustics* **117**, 370–377, The modelling of the opening and closure of a crack.
9. A. K. Pandey, M. Biswas and M. M. Samman 1991 *Journal of Sound and Vibration* **145**, 321–332. Damage Detection from change in curvature mode shapes.
10. P. F. Rizos, N. Aspragathos and A. D. Dimarogonas 1990 *Journal of Sound and Vibration* **138**, 381–388. Identification of crack location and magnitude in a cantilever beam from the vibration modes.
11. W. Q. Feng, K. Y. Zhang and X. Y. Wu 1989 *Proceedings of the VII International Modal Analysis Conference*, 1100–1108. Research on the change of modal parameters of a beam resulted from a slot.
12. A. S. J. Swamidas and Y. Chen 1995 *Journal of Sound and Vibration* **186**, 325–343. Monitoring crack growth through change of modal parameters.
13. C. P. Ratcliffe 1997 *Journal of Sound and Vibration* **204**, 505–517. Damage detection using a modified Laplacian operator on modal shape data.
14. F. D. Ju and M. E. Mimovich 1988 *Transactions of ASME* **110**, 456–463. Experimental diagnosis of fracture damage in structures by the modal frequency method.
15. T. C. Tasi and Y. Z. Wang 1996 *Journal of Sound and Vibration*, **192**, 607–620. Vibration analysis and diagnosis of a cracked shaft.
16. I. Chance, G. R. Tomilinson and K. Worden **19**, 770–785. IMAC, a simplified approach to the numerical and experimental modeling of the dynamics of a cracked beam.

APPENDIX: NOMENCLATURE

$A(x)$	cross-section area of the beam
B	breadth of the beam
E	Young's modulus
G	shear modulus
$I(x)$	moment of inertia of cross section
$J(x)$	polar moment of inertia
J_0	mass moment of inertia per unit length
L, l	length of the beam
l_0	crack location from fixed end
T	thickness of beam
U	strain energy
V	kinetic energy
f	forcing function
m	mass per unit length
n	mode number
w_n	bending mode shape of nth frequency
Δx	crack width
β_n	roots of nth mode shape function
λ	natural frequency squarer
ρ	density
θ_n	torsional mode shape nth frequency
ω	natural frequency